

Superconducting scanning tunneling microscopy tips in a magnetic field: Geometry-controlled order of the phase transition

Matthias Eltschka¹, Berthold Jäck, Maximilian Assig, Oleg V. Kondrashov, Mikhail A. Skvortsov, Markus Etzkorn, Christian R. Ast, and Klaus Kern

Citation: *Appl. Phys. Lett.* **107**, 122601 (2015); doi: 10.1063/1.4931359

View online: <http://dx.doi.org/10.1063/1.4931359>

View Table of Contents: <http://aip.scitation.org/toc/apl/107/12>

Published by the [American Institute of Physics](#)

Articles you may be interested in

[A nanoscale gigahertz source realized with Josephson scanning tunneling microscopy](#)

Appl. Phys. Lett. **106**, 013109013109 (2015); 10.1063/1.4905322



**FIND THE NEEDLE IN THE
HIRING HAYSTACK**

POST JOBS AND REACH THOUSANDS OF
QUALIFIED SCIENTISTS EACH MONTH.

PHYSICS TODAY | JOBS
WWW.PHYSICSTODAY.ORG/JOBS

Superconducting scanning tunneling microscopy tips in a magnetic field: Geometry-controlled order of the phase transition

Matthias Eltschka,^{1,a)} Berthold Jäck,¹ Maximilian Assig,¹ Oleg V. Kondrashov,² Mikhail A. Skvortsov,^{2,3,4} Markus Etzkorn,¹ Christian R. Ast,¹ and Klaus Kern^{1,5}

¹Max-Planck-Institut für Festkörperforschung, 70569 Stuttgart, Germany

²Moscow Institute of Physics and Technology, 141700 Moscow, Russia

³Skolkovo Institute of Science and Technology, 143026 Moscow, Russia

⁴L. D. Landau Institute for Theoretical Physics, 142432 Chernogolovka, Russia

⁵Institut de Physique de la Matière Condensée, Ecole Polytechnique Fédérale de Lausanne, 1015 Lausanne, Switzerland

(Received 17 July 2015; accepted 7 September 2015; published online 21 September 2015)

The properties of geometrically confined superconductors significantly differ from their bulk counterparts. Here, we demonstrate the geometrical impact for superconducting scanning tunneling microscopy (STM) tips, where the confinement ranges from the atomic to the mesoscopic scale. To this end, we compare the experimentally determined magnetic field dependence for several vanadium tips to microscopic calculations based on the Usadel equation. For our theoretical model of a superconducting cone, we find a direct correlation between the geometry and the order of the superconducting phase transition. Increasing the opening angle of the cone changes the phase transition from first to second order. Comparing our experimental findings to the theory reveals first and second order quantum phase transitions in the vanadium STM tips. In addition, the theory also explains experimentally observed broadening effects by the specific tip geometry. © 2015 AIP Publishing LLC. [<http://dx.doi.org/10.1063/1.4931359>]

When geometrically confined to dimensions smaller than the London penetration depth, superconductors in a magnetic field exhibit properties that can significantly differ from their bulk counterparts. For example, the critical magnetic fields, at which superconducting thin films become normal conducting, are considerably enhanced compared to the bulk due to geometrical confinement.^{1–4} At the critical field, the order of the superconducting phase transition also depends on geometrical factors such as the film thickness.^{3,4} In addition to thin films, various other geometries have been studied experimentally and theoretically such as disks, rings, or spheres.^{5–10} A cone presents a particularly interesting and challenging geometry covering length scales from the atomic scale apex to the macroscopic base.¹¹ At mesoscopic length scales where superconductivity has to be described, cones are a highly suitable approximation for superconducting tips in scanning tunneling microscopy (STM). Superconducting STM tips can be employed for enhancing the energy resolution (e. g. Refs. 12 and 13), for accessing parameters of a superconductor,¹⁴ as probes for absolute spin polarization,¹⁵ or for designing Josephson junctions.^{16–18} In a conical geometry, it is *a priori* not clear if the superconducting properties are affected due to the mesoscopic confinement or if quantum size effects have to be considered as in zero-dimensional (0D) superconductors.^{19–22} In this context, the magnetic field dependence of the superconducting gap is of fundamental interest. The order of the superconducting phase transition also remains an open question. Therefore, it is essential to understand the impact of the confinement on tunneling experiments employing superconducting STM tips.

Here, we investigate the influence of the geometry on the superconducting phase transition of STM tips in magnetic fields. To this end, we measure the magnetic field dependence of several vanadium tips by STM and use the Usadel equation for modeling the tips as sharp superconducting cones in magnetic fields. Comparing our experimental results with the calculations, we characterize the order of the superconducting phase transitions in the V tips. We find that we can tune the order of the phase transition by changing the geometry of the tip apex, i.e., first order transitions for sharp tips and second order transitions for blunt tips. Furthermore, our approach allows to correlate experimentally observed broadening effects to the geometric confinement of the superconductor.

Fig. 1(a) shows differential conductance (dI/dV) tunneling spectra of a superconducting V tip on single crystal V(100) as a function of magnetic field B and at a temperature of 15 mK.^{23,29} Since the critical field for bulk V $B_{c,bulk} < 0.5$ T, the sample is normal conducting for all measurements shown. The dI/dV -spectra show the superconducting quasi-particle density of states (DOS) of the STM tip up to its critical field B_c of about 4.2 T, which is higher than in the bulk due to the dimensional confinement near the apex.¹⁵ The lifted spin degeneracy results in the characteristic four-peak-structure of the superconducting coherence peaks.²⁴

To characterize our data, we start with the simplest 0D model of a small superconductor in a magnetic field. In this model analyzed by Maki,^{25,26} the DOS is given by

$$\rho_{\uparrow}(E) = (\rho_0/2)\text{sgn}(E)\text{Re}\left\{u_{\pm}/\sqrt{u_{\pm}^2 - 1}\right\}, \quad (1)$$

where u_+ and u_- are implicitly defined by

^{a)}Author to whom correspondence should be addressed. Electronic mail: m.eltschka@fkf.mpg.de

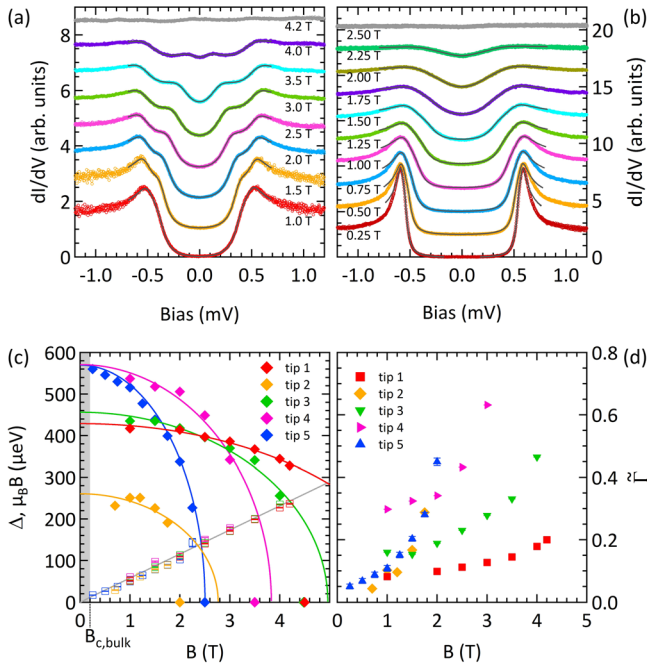


FIG. 1. Superconducting vanadium STM tips in external magnetic fields. (a) The dI/dV spectra are measured with a superconducting V tip on normal conducting samples at 15 mK. With increasing external magnetic field, the Zeeman splitting increases and the superconducting gap decreases. The lines are fits based on the extended Maki model (EMM). (b) The spectral features of another V tip appear much broader indicating the influence of the specific tip geometry. (c) Superconducting gaps Δ (solid markers) and Zeeman energy $\mu_B B$ (open markers) are fit results of several tips. The lines indicate elliptic fits of the superconducting gaps at small B . (d) The reduced parameter $\tilde{\Gamma} = \Gamma/\Delta$ takes spectral broadening into account.

$$u_{\pm} = \frac{(E - i\Gamma) \mp \mu_B B}{\Delta} + \zeta \frac{u_{\pm}}{\sqrt{1 - u_{\pm}^2}} + b \frac{u_{\mp} - u_{\pm}}{\sqrt{1 - u_{\pm}^2}}, \quad (2)$$

with ρ_0 is the normal conducting DOS, E is the energy, μ_B is the magnetic moment (Bohr magneton), Δ is the superconducting order parameter, ζ is the orbital depairing parameter, B is the external magnetic field, and b is the spin-orbit scattering parameter. In our dI/dV spectra, we usually observe broader spectral features than expected just from thermal effects ($T = 15$ mK). At higher magnetic fields, we observe the filling of the superconducting gap where the dI/dV -signal does not completely go to zero as predicted by the original Maki's model.^{25,26} Therefore, we employ an extended Maki's model (EMM) with an additional phenomenological broadening parameter Γ .²⁷ Including Γ broadens the spectral features and results in a much better fit to our experimental data. We emphasize that an artificially introduced parameter Γ should not be attributed to any real pair-breaking mechanism. Its appearance is the price to pay for a good fitting of experimental data by an oversimplified 0D Maki's model. Below, we present a consistent microscopic description for our experimental data based on the Usadel equations.

In Fig. 1(a), the black solid lines represent fits to the data using the EMM with $b = 0.10 \pm 0.04$ (which is in good agreement with Ref. 28) and a magnetic field dependent ζ (for details see Ref. 29). In Fig. 1(b), the same experiment is repeated with a different V tip. While the superconducting DOS of the tip is clearly visible and similar to Fig. 1(a), the spectral features appear much broader and the critical field

$B_c \approx 2.5$ T is smaller. Fitting the more broadened spectra with the EMM requires larger Γ values than in Fig. 1(a).

Repeating these experiments for several V tips (made from five different pieces of V wire), we extract the superconducting parameters by the fitting routine based on the EMM. Fig. 1(c) shows the superconducting gap Δ (solid symbols) and the Zeeman energy (open symbols) as a function of the external magnetic field B . The analysis reveals large variations of the critical fields ($2 \text{ T} \leq B_c \leq 4.5 \text{ T}$) as well as of the superconducting gaps at zero field ($260 \mu\text{eV} \leq \Delta_0 \leq 580 \mu\text{eV}$). The observed Zeeman splitting follows the theoretical prediction of a system with spin $s = 1/2$ and $g = 2$ for all investigated V tips [gray line in Fig. 1(c)].³⁰

Further, the behavior of the superconducting gap Δ in the magnetic field depends on the specific tip (cf. Fig. 1(c)). While tip 1 shows a discontinuous transition to the normal state at high fields, other tips, such as tip 5, show a more continuous phase transition at lower fields. This behavior becomes more obvious when comparing the measured superconducting gaps to ellipses drawn as a guide to the eye in Fig. 1(c). We further find different initial superconducting gaps Δ_0 at zero field, all of which are smaller than the superconducting bulk gap of V ($\Delta_{0,\text{bulk}} = 820 \mu\text{eV}$ at $T = 0$ K).³¹ This reduction might be explained by the influence of vanadium oxide at the tip surface, changes in the phonon dispersion, and correspondingly the electron-phonon interaction, or grain size effects within the material.³²⁻³⁴ The parameter Γ obtained by fitting the experimental spectra within the EMM is shown in Fig. 1(d), where $\tilde{\Gamma} = \Gamma/\Delta$ is plotted as a function of the external magnetic field. The values of $\tilde{\Gamma}$ increase monotonically with the field for all V tips. Both $\tilde{\Gamma}$ as well as the rate of change $d\tilde{\Gamma}/dB$ depend on the specific tip, indicating that Γ is correlated with the specific geometry of each tip.

For a quantitative description of the non-uniform superconducting state in the V tips, we employ a quasi-classical approach based on the Usadel equation.³⁵ This approach is suitable for the polycrystalline V tips in the dirty limit, where the electron mean free path l is smaller than the coherence length. We model the STM tips as superconducting cones with the opening angle α in an external magnetic field B applied along the tip axis (z -direction) [see insets Figs. 2(a) and 2(b)]. For sharp tips ($\alpha \ll 1$), one can use the adiabatic approximation neglecting variations perpendicular to the cone axis.¹⁵ The resulting one-dimensional (1D) Usadel equation is written in terms of the spectral angle $\theta_{\epsilon}(\tilde{z})$ ^{29,36}

$$\frac{\alpha/\alpha_c}{3\sqrt{2}} \mu_B B \left(-\theta'_{\epsilon} - \frac{2}{\tilde{z}} \theta'_{\epsilon} + \tilde{z}^2 \sin 2\theta_{\epsilon} \right) + (\epsilon \pm i\mu_B B) \sin \theta_{\epsilon} = \Delta(\tilde{z}) \cos \theta_{\epsilon}, \quad (3)$$

where ϵ is the imaginary Matsubara energy, \tilde{z} is the dimensionless z -coordinate defined by $\tilde{z} = z\sqrt{\pi B \alpha / 2\Phi_0}$, $\Phi_0 = h/2e$ is the superconducting flux quantum, and \pm refers to the spin orientation. The critical angle α_c (described in more detail below) is defined as

$$\alpha_c = (2\sqrt{2}/3)(c\mu_B/eD) = \sqrt{2}(m_*/m)/(k_F l) \ll 1, \quad (4)$$

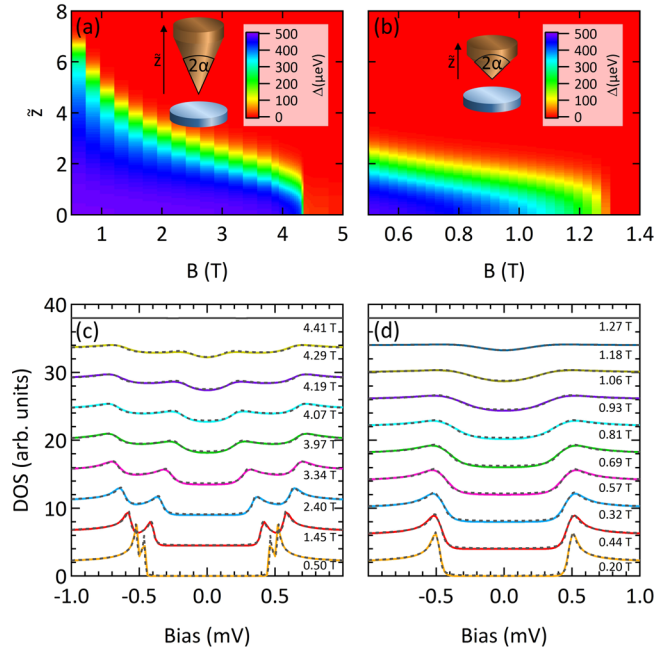


FIG. 2. Calculated superconductivity of cones with opening angle α in an external magnetic field. (a) The apex of a sharp cone ($\alpha/\alpha_c = 0.4$) remains superconducting for magnetic fields up to 4.35 T. (b) For a blunt cone ($\alpha/\alpha_c = 3.2$), the superconducting part is more confined to the apex and the critical field is smaller ($B_c = 1.27$ T). (c) The DOS of the sharp tip ($\alpha/\alpha_c = 0.4$) exhibits clear spectral features, and the lifted spin degeneracy is clearly visible due to the Zeeman energy. (d) The DOS of the blunt tip ($\alpha/\alpha_c = 3.2$) appears more broadened.

with the speed of light c , the diffusion coefficient D , the Fermi wave vector k_F , the electron mass m , and the effective mass m_* . The order parameter $\Delta(\vec{z})$ is determined from the self-consistency equation at $T = 0$

$$\Delta(\vec{z}) = \lambda \operatorname{Re} \int_0^{\hbar\omega_D} \sin \theta_\epsilon(\vec{z}) d\epsilon, \quad (5)$$

where λ is Cooper-channel interaction constant, and $\hbar\omega_D$ is the Debye energy. The DOS is obtained by analytic continuation

$$\rho_{\uparrow\downarrow}(E, \vec{z}) = (\rho_0/2) \operatorname{sgn}(E) \operatorname{Re} \cos \theta_{-iE}^\pm(\vec{z}), \quad (6)$$

where $\theta_\epsilon^\pm(\vec{z})$ refers to the spin orientation in Eq. (3). With $u_\pm = -i \coth \theta^\pm$, Eq. (6) generalizes Eq. (1) to a non-uniform case.

Calculating the free energy of such a system reveals that the nature of the quantum phase transition at the critical field is determined by the ratio α/α_c . While for small opening angles $\alpha < \alpha_c$ (sharp tips), a first order phase transition with abrupt disappearance of Δ at $B = B_c$ is expected, larger opening angles $\alpha > \alpha_c$ (blunter tips) exhibit a second order phase transition, with Δ continuously vanishing at $B = B_c$.²⁹

In Figs. 2(a) and 2(b), the superconducting gap in a tip with $\alpha/\alpha_c = 0.4$ and 3.2 is displayed, respectively, as a function of the dimensionless coordinate \bar{z} . The figures show that only the apex of the cone remains superconducting in an external magnetic field $B > B_{c,\text{bulk}}$. Increasing the field shrinks the superconducting region, which becomes more confined to the apex. At a critical field B_c of 4.35 T in (a) and 1.27 T in (b), the superconducting gap vanishes and the whole cone is normal conducting. This demonstrates a strong

influence of the confined geometry, i.e., the opening angle α . The geometrical confinement also affects the quasi-particle DOS measured in tunnel experiments. In Figs. 2(c) and 2(d), the calculated quasi-particle DOS at the apex of a superconducting cone is displayed for $\alpha/\alpha_c = 0.4$ and 3.2, respectively, for different external magnetic fields. The spectral features are well-defined and the increasing Zeeman splitting is clearly observable in (c), while in (d), the wider opening angle results in broadened features with the spin-up and spin-down contributions completely smeared out.

Due to the high computational cost related with the self-consistency equation Eq. (5), the Usadel approach is unsuitable as fitting routine for the experimental dI/dV -spectra. To establish the relation between the microscopic theory and the phenomenological EMM, we employ the latter (now with $b = \zeta = 0$) to fit the calculated spectra [dashed lines in Figs. 2(c) and 2(d)]. The superconducting gaps obtained from the EMM fits match the results obtained from the Usadel equation.

In Fig. 3(a), the magnetic field dependence of the superconducting gap Δ is presented for several superconducting cones with varying opening angles $0.2 \leq \alpha/\alpha_c \leq 4$. Increasing α/α_c clearly decreases the critical field B_c of the cone. More importantly, at the critical field, the ratio α/α_c determines the order of the superconducting phase transition. Sharp cones with $\alpha/\alpha_c < 1$ exhibit a first order phase transition to the normal state. For $\alpha/\alpha_c < 1$, Δ only decreases slowly up to the critical field where it abruptly vanishes and the cone becomes normal. Blunter tips with $\alpha/\alpha_c > 1$ (but still $\alpha \ll 1$) undergo a second order phase transition, in which the superconducting gap continuously decreases to zero. For a quantitative analysis of the spectral broadening, Fig. 3(b) shows the reduced broadening parameter $\tilde{\Gamma} = \Gamma/\Delta$ of the calculated quasi-particle DOS fitted by the EMM as a function of the magnetic field. For all cones with opening angles $0.2 \leq \alpha/\alpha_c \leq 4$, the spectral broadening is well-described by the phenomenological parameter Γ . More importantly, the rate of change $d\tilde{\Gamma}/dB$ in the magnetic field is also a function of the opening angle. When increasing α/α_c , the spectral broadening becomes more sensitive to the external field, and therefore, the observation of features such as coherence peaks split by the Zeeman energy is more difficult.

For comparing the results obtained from the Usadel equation to our experimental findings in Fig. 4(a), we normalize

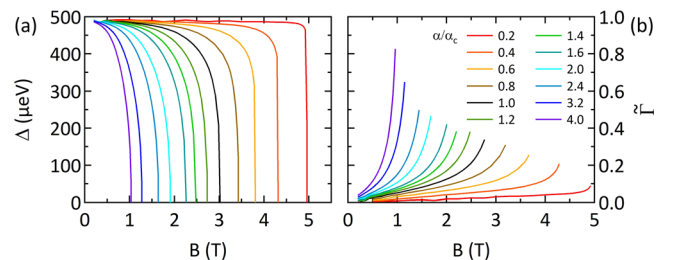


FIG. 3. Superconducting parameters extracted by the EMM fit of the Usadel spectra. (a) The magnetic field dependence of the superconducting gap Δ is determined by the opening angle α . For $\alpha/\alpha_c < 1$, the phase transition is of first order, and for $\alpha/\alpha_c > 1$ a second order phase transition is observed. (b) The spectral broadening is described by the parameter $\tilde{\Gamma} = \Gamma/\Delta$, which increases with α .

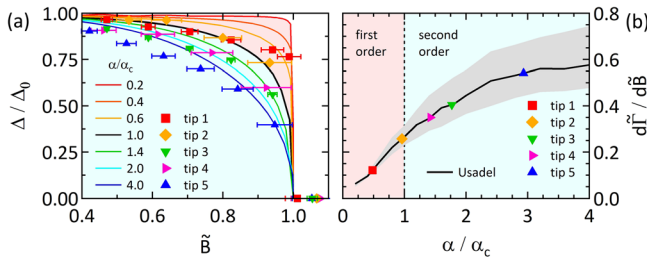


FIG. 4. Comparison of the Usadel calculations and the experimental results. (a) The normalized superconducting gaps Δ/Δ_0 calculated by the Usadel equation (lines) as a function of the normalized magnetic field $\tilde{B} = B/B_c$ exhibit first and second order phase transition depending on the opening angle α . The markers are the normalized experimental data from Fig. 1(c). (b) The rate of change of the normalized broadening parameter $\tilde{\Gamma}$ in the normalized magnetic field \tilde{B} allows for an additional classification of the superconducting phase transition in the V tips.

the measurements and calculations to the zero-field gaps Δ_0 and critical fields B_c . The black line for $\alpha/\alpha_c = 1$ marks the separation between phase transitions of first and second order. The superconducting gaps of tip 1 lie in the region above the separation line and, therefore, tip 1 undergoes a phase transition of first order. For tip 2, the classification of the phase transition is ambiguous, since it is too close to the line $\alpha/\alpha_c = 1$. Tips 3–5 exhibit a second order phase transition as already indicated by the continuously vanishing gaps [Fig. 1(c)]. In Fig. 4(b), the rate of change $d\tilde{\Gamma}/d\tilde{B}$ in the normalized magnetic field ($\tilde{B} = B/B_c$) is calculated for the Usadel results at lower magnetic fields ($0.5B_c \leq B \leq 0.7B_c$), where a linear approximation is reasonable. The gray area indicates the results obtained when shifting the fitting range to $0.45B_c \leq B \leq 0.65B_c$, respectively, to $0.55B_c \leq B \leq 0.75B_c$ and gives an error estimation for this approach. $d\tilde{\Gamma}/d\tilde{B}$ is also extracted from the fits of the experimental data for the similar field range. Comparing the experimentally obtained values of $d\tilde{\Gamma}/d\tilde{B}$ to the Usadel calculations [line in Fig. 4(b)] allows for estimating an effective α/α_c . This approach provides an additional independent parameter to characterize the order of the superconducting phase transition. Again, it shows that tip 1 undergoes a first order phase transition, while tip 2 cannot unambiguously be characterized. Tips 3–5 are clearly in the regime with $\alpha/\alpha_c > 1$ resulting in second order phase transitions. Therefore, the behavior of the broadening parameter confirms the characterization of the phase transition by the superconducting gaps [Fig. 4(a)].

In conclusion, we have investigated the quantum phase transitions of superconducting V STM tips of various geometries in magnetic fields. Solving an effective 1D Usadel equation, we have demonstrated the direct correlation of the cone geometry and the order of the superconducting phase transition: first order for very sharp tips ($\alpha < \alpha_c$) and second order for blunter tips ($\alpha > \alpha_c$). Our microscopic approach provides a physical interpretation for the experimentally observed broadening of the dI/dV spectra and sheds light on the origin of the phenomenological parameter Γ introduced to fit the data by the very simple Maki model. This parameter is not related to any pair-breaking but is a formal way to remedy the inapplicability of the 0D Maki model to systems with nonuniform superconductivity. For experimental applications, a detailed understanding of

the superconductivity in the cone geometry is essential. Our study facilitates the application of superconducting STM tips in presence of an external magnetic field as additional tuning parameter, which enables techniques such as Meservey-Tedrow-Fulde STM (MTF-STM) or Josephson STM.^{15,16,18,37} Both techniques greatly benefit from clearly distinguishable spectral dI/dV features, e.g., for resolving the Zeeman splitting and probing absolute spin polarization in MTF-STM. The combination of Josephson STM with external magnetic fields enables a wide range of additional experiments, such as single electron spin resonance measurements.³⁸ Our findings suggest that both techniques benefit from superconducting tips with small opening angles ($\alpha \ll 1$) resulting in small broadening ($\Gamma \ll \Delta$) and first order phase transitions at high critical fields ($B_c \gg B_{c,\text{bulk}}$).

C.R.A. acknowledges funding from the Emmy-Noether-Program of the Deutsche Forschungsgemeinschaft (DFG). Research by M.A.S. was supported in part by the RFBR Grant No. 13-02-01389.

- ¹I. Giaever and K. Megerle, *Phys. Rev.* **122**, 1101 (1961).
- ²P. Townsend and J. Sutton, *Phys. Rev.* **128**, 591 (1962).
- ³D. H. Douglass and R. Meservey, *Phys. Rev.* **135**, A19 (1964).
- ⁴R. Meservey and D. H. Douglass, *Phys. Rev.* **135**, A24 (1964).
- ⁵P. S. Deo, V. A. Schweigert, F. M. Peeters, and A. K. Geim, *Phys. Rev. Lett.* **79**, 4653 (1997).
- ⁶A. Kanda, B. J. Baelus, F. M. Peeters, K. Kadowaki, and Y. Ootuka, *Phys. Rev. Lett.* **93**, 257002 (2004).
- ⁷R. Benoit and W. Zwerger, *Z. Phys. B* **103**, 377 (1997).
- ⁸A. S. Mel'nikov and V. M. Vinokur, *Nature* **415**, 60 (2002).
- ⁹G.-Q. Zha, S.-P. Zhou, B.-H. Zhu, Y.-M. Shi, and H.-W. Zhao, *Phys. Rev. B* **74**, 024527 (2006).
- ¹⁰B. J. Baelus, D. Sun, and F. M. Peeters, *Phys. Rev. B* **75**, 174523 (2007).
- ¹¹Y. Chen, M. M. Doria, and F. M. Peeters, *Phys. Rev. B* **77**, 054511 (2008).
- ¹²S. H. Pan, E. W. Hudson, and J. C. Davis, *Appl. Phys. Lett.* **73**, 2992 (1998).
- ¹³K. J. Franke, G. Schulze, and J. I. Pascual, *Science* **332**, 940 (2011).
- ¹⁴A. Kohen, T. Proslie, T. Cren, Y. Noat, W. Sacks, H. Berger, and D. Roditchev, *Phys. Rev. Lett.* **97**, 027001 (2006).
- ¹⁵M. Eltschka, B. Jäck, M. Assig, O. V. Kondrashov, M. A. Skvortsov, M. Eitzkorn, C. R. Ast, and K. Kern, *Nano Lett.* **14**, 7171 (2014).
- ¹⁶O. Naaman, W. Teizer, and R. C. Dynes, *Phys. Rev. Lett.* **87**, 097004 (2001).
- ¹⁷J. G. Rodrigo, H. Suderow, and S. Vieira, *Eur. Phys. J. B* **40**, 483 (2004).
- ¹⁸B. Jäck, M. Eltschka, M. Assig, A. Hardock, M. Eitzkorn, C. R. Ast, and K. Kern, *Appl. Phys. Lett.* **106**, 013109 (2015).
- ¹⁹V. Kresin and Y. Ovchinnikov, *Phys. Rev. B* **74**, 024514 (2006).
- ²⁰A. García-García, J. Urbina, E. Yuzbashyan, K. Richter, and B. Altshuler, *Phys. Rev. Lett.* **100**, 187001 (2008).
- ²¹H. Olofsson, S. Åberg, and P. Leboeuf, *Phys. Rev. Lett.* **100**, 037005 (2008).
- ²²S. Bose, A. M. García-García, M. M. Ugeda, J. D. Urbina, C. H. M. I. Brihuega, and K. Kern, *Nat. Mater.* **9**, 550 (2010).
- ²³M. Assig, M. Eitzkorn, A. Enders, W. Stiepany, C. R. Ast, and K. Kern, *Rev. Sci. Instrum.* **84**, 033903 (2013).
- ²⁴R. Meservey, P. M. Tedrow, and P. Fulde, *Phys. Rev. Lett.* **25**, 1270 (1970).
- ²⁵K. Maki, *Prog. Theor. Phys.* **32**, 29 (1964).
- ²⁶D. C. Worledge and T. H. Geballe, *Phys. Rev. B* **62**, 447 (2000).
- ²⁷R. C. Dynes, V. Narayanamurti, and J. P. Garno, *Phys. Rev. Lett.* **41**, 1509 (1978).
- ²⁸P. Tedrow and R. Meservey, *Phys. Lett. A* **69**, 285 (1978).
- ²⁹See supplementary material at <http://dx.doi.org/10.1063/1.4931359> for theoretical description.
- ³⁰G. A. Gibson and R. Meservey, *Phys. Rev. B* **40**, 8705 (1989).
- ³¹S. T. Sekula and R. H. Kernohan, *Phys. Rev. B* **5**, 904 (1972).

³²W. L. McMillan, *Phys. Rev.* **167**, 331 (1968).

³³T. T. Chen, J. T. Chen, J. D. Leslie, and H. J. T. Smith, *Phys. Rev. Lett.* **22**, 526 (1969).

³⁴M. Strongin, R. S. Thompson, O. F. Kammerer, and J. E. Crow, *Phys. Rev. B* **1**, 1078 (1970).

³⁵K. D. Usadel, *Phys. Rev. Lett.* **25**, 507 (1970).

³⁶D. A. Ivanov, Y. V. Fominov, M. A. Skvortsov, and P. M. Ostrovsky, *Phys. Rev. B* **80**, 134501 (2009).

³⁷H. Kimura, R. P. Barber, S. Ono, Y. Ando, and R. C. Dynes, *Phys. Rev. Lett.* **101**, 037002 (2008).

³⁸A. V. Balatsky, M. Nishijima, and Y. Manassen, *Adv. Phys.* **61**, 117 (2012).